THE EFFECTS OF THERMAL BARRIER COATINGS ON DIESEL ENGINE EMISSIONS

A.L. Boehman, M. Vittal, J. Borek, and D. Marks - The Pennsylvania State University

D. A. Okrent, Rupprecht & Patashnick Co., Inc. and A.P. Bentz, JBL Associates, Inc.

INTRODUCTION

The major promises of thermal barrier coated (also known as low heat rejection, LHR) engines were increased thermal efficiency and elimination of the cooling system [1]. A simple first law of thermodynamics analysis of the energy conversion process within a diesel engine would indicate that if heat rejection to the coolant was eliminated, the thermal efficiency of the engine could be increased. However, due to a number of challenges posed by the presence of thermal barrier coatings within the engine, these particular promises have not been kept.

What instead appears to be the benefit of thermal barrier coatings is a change in smoke and particulate emissions [2-5]. The effect on NO_x emissions is not as clear, with some investigations showing increases in NO_x emissions and others showing no increase. Also, a fuel economy penalty can be expected with a thermal barrier coated diesel engine. But, as a strategy to reduce particulate emissions, thermal barrier coatings have proven to be effective, especially in some recent studies by Engelhard Corp. [4] and at Penn State [5-7].

In this paper, we summarize some our of recent work at Penn State that has been performed on behalf of the U.S. Coast Guard R&D Center, Groton, CT. This work has included collaboration with Rupprecht & Patashnick Co. (R&P Co.), Inc., Albany, NY. Here we will briefly describe the experimental configuration used, and some of the key results obtained thus far. The motivation for this work has been to determine whether rebuilding in-service marine diesel engines to include thermal barrier coated parts is a viable means of reducing emissions from Coast Guard vessels. Objectives of this work have been to characterize changes in emissions caused by thermal barrier coatings and to understand the reasons for any observed changes.

EXPERIMENTAL

Apparatus and Testing Procedure:

A schematic of the engine test cell is shown in Figure 1 and specifications of this engine are listed in Table 1. As seen in the figure, the engine was coupled to a Clayton water brake dynamometer. The dynamometer torque was measured using a strain gauge load cell and the speed was monitored using a 60-tooth gear assembly. The exhaust, lube oil and coolant temperatures were also measured to monitor engine operation. The temperature of the ex-haust gas was monitored with a type-K thermocouple mounted in the exhaust manifold. The data acquisition system was a Gateway 2000 P-5/100 MHZ computer with a DAS-8/PGA data acquisition and control board from Keithley Metrabyte. The computer was set up to log real-time engine speed, engine torque, engine power, and exhaust, lube oil and coolant temperatures.

The piston crown, cylinder head, and valves were given thin thermal barrier coatings (300 μm thick) by Turbine Components Corporation of Branford, CT. The parts were given a bond coat of NiCoCrAly, followed by a top coat of Metco pre-alloyed, yttria stabilized zirconia. No attempt was made to maintain a fixed compression ratio. Instead identical engine components were used where the only difference was the presence of the ceramic coating on the aforementioned surfaces. Assuming that the combustion chamber consists of a simple cylindrical surface, we estimate that the compression ratio changed from 19.5 to 21.6 between the baseline and ceramic coated configurations. However, the actual difference in compression ratio was most likely negligible. The baseline (uncoated) engine acquired a significant carbon deposit during the break-in period, which would increase the baseline compression ratio. The Coordinating Research Council considers a "trace to light" combustion chamber deposit to be of 200 to 400

μm thickness [8]. During the break-in period, the ceramic coated surfaces resisted formation of significant carbon deposits. So, the "in-use" compression ratios of the baseline and ceramic coated engines were probably similar. If the carbon deposit on the baseline engine increased to even a "medium" rating (1.59 mm), the ceramic coated engine could result in lower "in use" compression ratio.

The test procedure was chosen so as to match the typical duty cycle of a diesel engine for marine applications. The International Standard (ISO 8178, Part 4) was consulted for guidance. Table 2 shows the test matrix used in this work. It is based broadly on cycle E3 (Marine Applications, heavy-duty propulsion engines) described in ISO 8178, Part 4. There are four modes, a mode being a part of the test cycle with defined speed and torque.

A protocol was established to effect the changeover from the baseline (metal) configuration to the ceramic-coated configuration. The same piston rings and fuel injector were used for both configurations. However, for each changeover, the cylinder head gasket was replaced with a new (identical) gasket to ensure quality of the seal between the head and the cylinder block. The lube oil and coolant were also changed, although lubricant consumption was not monitored. The lube oil was SAE 10W30 Motor Oil from Valvoline and the coolant was Prestone Antifreeze/Coolant. Each time the lube oil was changed, the engine was run for 8 hours to break in the new oil. The oil temperature in the engine typically took up to an hour to reach steady state. Thus, an hour-long warm-up period was always used to prepare the engine for testing. A low-sulfur Diesel fuel from BP Oil was used in all tests.

The gaseous portion of the exhaust was analyzed using an ENERAC Model 3000E Integrated Emissions System and a NICOLET Magna-IR 550 Spectrometer. The ENERAC gas analyzer is based on electrochemical sensors and measures NO, NO_2, CO, combustibles, SO_2 and O_2 concentrations. The FTIR was used to quantify CO, NO, NO_2 and N_2O emissions.

Diesel exhaust particulates were collected on Pallflex TX40HI20WW filters using a Sierra Instruments Model BG-1 Micro-Dilution Test Stand. The total flow rate was set at 50.0 standard liters/minute (SLPM) and the dilution flow rate was set at 41.7 SLPM. These settings yield a sample flow rate of 8.3 SLPM and thus a dilution ratio of 5.0. Particulates were collected for ten minutes at each mode. The International Standard (ISO/DIS 8178-1.2) stipulates that the temperature of the collection filters should be below 52° C, a minimum of 2.3 mg of soot should be collected, the pressure drop increase during the test should not exceed 25 kPa, and the filters should not tear. The flow rates were adjusted by trial and error until these criteria were satisfied completely. All runs reported here complied with these requirements. Particulate was collected on the primary filter and the secondary filter served as a back up to collect any particulate that should pass through the primary filter. Before and after sampling, the filters were allowed to equilibrate in a humidity-controlled chamber and weighed using a Sartorius microbalance with an accuracy of ±2 μg.

Several methods were used to study the chemical and physical characteristics of the particulate matter collected from the baseline and ceramic coated engine over the four modes of the Type E3 test. These were scanning electron microscopy (SEM), electron dispersive spectrometry

Table 2. ENGINE TEST MATRIX

	Mode 1	Mode 2	Mode 3	Mode 4
Speed (RPM)	2200	2002	1760	1386
% Rated Speed	100	91	80	63
Power (HP)	12.26	8.77	5.32	2.03
% Rated Power	81.7	58.5	35.5	13.5

Table 1. ENGINE SPECIFICATIONS

Parameter	Type / Value
Make	Yanmar
Model	TS180C
Type	Prechamber
No. of cylinders	1
Bore * stroke (mm)	102*106
Displacement (l)	.866
Continuous rating output (kW/rpm)	11.2/2200
Specific Fuel Consumption (g/kWh)	275
Compression ratio	19.5

(EDS), thermal analysis, and GC, GC-MS, and HPLC analyses of the soluble fraction. At present, the chemical analyses of the SOF are only qualitative, and will not be discussed here. Efforts to complete a quantitative analysis procedure will likely make use of HPLC, since this provided superior sensitivity and peak identification for PAH compounds.

SEM and EDS Analyses:
An ISI SX 40-ABT SEM was used for energy dispersive X-ray analyses and a JOEL JSM-6300 FV SEM was used for microstructural analyses. The particulate laden Pallflex filters were dried for 1 hr. at 80°C under vacuum to remove moisture. This reduced the volatility of the particulate samples and enhanced the stability of the SEM probe and imaging system. Small quantities of particulate matter were placed on test stands to permit the SEM analysis. For the ISI SEM, a carbon test stand was used. For the JEOL SEM, an aluminum test stand was used. In both situations, a vacuum safe double-sided adhesive tape was used to mount the particulate samples on the test stands. In order to take photographs with the scanning electron microscopes, it was necessary to coat the samples with gold, a conducting medium, by using a sputter coater.

Thermal Analysis:
A Series 5100 Diesel Particulate Measurement System from R&P Co. was attached to the exhaust stack by means of a heated sample tube. The instrument cycle has two phases which are controlled by an instrument computer. During the collection phase, the system draws a sample of particulate-laden gas from the exhaust and routes it to a quartz filter. As the gas passes through the filter, particulate is trapped and filtered exhaust gas is vented out of the device. During the analysis phase, the collected sample is heated according to a user-defined temperature program. As the filter temperature increases, volatiles leave the filter, enter the gas stream, and travel to an afterburner set for 750° C. Oxidation of the carbonaceous materials produces CO_2, which is read by an NDIR CO_2 analyzer. The instrument computer converts the reading into a carbon concentration (mg of carbon per ml of exhaust gas collected).

The collection and analysis parameters used in this work were as follows: Particulate-laden exhaust gas was sampled at a rate of 8.0 liters/min for 60 sec at engine operating modes 1 and 2, and 120 sec at modes 3 and 4. The collection temperature was 75° C. After collection, the filter temperature was ramped from 200° to 750° C at a rate of 5° C/min. The CO_2 concentration data at each temperature were downloaded from the instrument to a PC for graphing.

RESULTS AND DISCUSSION

Emissions Measurements:
Emissions of CO and NO_x exhibited the same trends for both the baseline and ceramic-coated engines. As shown in Fig. 2, brake specific CO emissions decreased sharply from Mode 4 to Mode 3, and slightly thereafter. Brake specific NO_x emissions decreased with increasing power

as shown in Fig. 3. For all modes, CO emissions were higher for the ceramic-coated engine, while NO_x emissions were the same for both configurations. The exhaust temperature was higher for the ceramic-coated engine over the full range of power settings.

It was expected that CO emissions would be lower for the ceramic-coated engine since the higher temperatures of the combustion gas and chamber walls should increase the rate of oxidation reactions leading to the complete combustion product, CO_2 [9]. However, for all modes there was a slight increase in BSCO emissions for the ceramic-coated engine. Higher CO concentrations were also reported by researchers at the Southwest Research Institute [10] for an LHR engine at high loads. One explanation lies in the strong relationship between CO emissions and the air/fuel ratio. As the air/-fuel ratio decreases, CO emissions increase. Exhaust gas analysis showed that for all modes the air/fuel ratio was lower for the ceramic-coated engine, thus explaining the higher CO concentrations in the exhaust. However, the sharp increase in BSCO emissions at Mode 4 for both configurations is harder to explain. Since diesel engines always operate on the lean side of stoichiometric, CO emissions should vary little with air/fuel ratio. It is possible that combustion at this mode was highly degraded because of lower temperatures resulting in slower kinetics.

The thermal barrier coating caused no significant change in the brake specific NO_x emissions. There was a marked decrease in $BSNO_x$ as power was increased. It may be expected that the ceramic-coated engine would have higher NO_x emissions due to the higher combustion temperatures and indeed other researchers have found an increase in NO_x emissions for LHR engines [3]. However, NO_x emissions are a function of both temperature and pressure of the burned gas. On the one hand, NO_x formation is accelerated by the higher temperatures in the LHR engine. On the other hand, the shift from premixed to diffusion combustion in the LHR engine results in lower peak pressures [1]. Due to these two competing factors, there may be a trade-off between the temperature and pressure effects on the NO_x formation rate. The most likely explanation for the observed consistency in NO_x emissions from the baseline and ceramic coated engine arises from the IDI engine configuration. As noted by Heywood [12], most of the NO forms within the prechamber and is then transported into cylinder where the NO concentration is frozen through rapid mixing with the surrounding air. The prechamber was not given a TBC coating, and thus, with regard to NO_x emissions, the opportunity for differences to arise between the two engine configurations was reduced.

The EPA defines particulates as solid or liquid except for water that collects on a filter at or below 52o C [13]. Diesel particulates are made up primarily of carbonaceous soot with some adsorbed hydrocarbons. Particulate formation in diesel engines is a complex and not fully understood process. From what is known, soot formation can be considered to occur in four stages: nucleation, surface growth, agglomeration, and adsorption/condensation [12]. The mass of soot in the exhaust gas is a function of the relationship between formation and oxidation. Both formation and oxidation rates are increased in the coated engine due to the higher temperatures and improved air to fuel mixing [14]. In the case of most LHR engines, the increase in oxidation rate is greater than the increase in formation rate. The higher oxidation rate led to decreased BS particulates in the ceramic-coated engine as shown in Fig. 4. At light loads (Modes 3 and 4) the decrease in particulate emissions from the ceramic-coated engine relative to the baseline engine was greater than at high loads (Modes 1 and 2). This is because at light loads a greater fraction of the fuel energy is lost to the coolant [13]. Thus, the decrease in energy rejection to the coolant due to the ceramic coating is greater at lighter loads, and a larger decrease in particulate emissions is realized.

EDS Analysis of Particulates:
For the uncoated engine, the energy dispersive X-ray analysis showed that in addition to a large amount of carbon © in the particulate sample; there was evidence of sulfur (S) and oxygen (O). There were also other elements present that were less than approximately three weight percent. These trace or minor elements were protactinium (Pa), titanium (Ti), zinc (Zn), calcium

(Ca), tellurium (Te), barium (Ba), cesium (Cs), sodium (Na), aluminum (Al), potassium (K), polonium (Po), chlorine (Cl), molybdenum (Mo), iron (Fe), and lead (Pb). For the coated engine, the energy dispersive X-ray analysis showed traces of nickel (Ni), yttria (Y), chromium (Cr), and cobalt (Co) in addition to those elements observed in the analysis of the particulate matter from the uncoated engine. The emission of several of the observed elements was likely the result of different factors such as utilization of organo-metallic additives in the diesel fuel or lubrication oil, contamination of the diesel fuel by alkyllead compounds, wear and corrosion of engine, and exhaust system parts [12]. Sulfur and traces of calcium iron, silicon, and chromium are found in diesel fuel; zinc, phosphorus, and calcium compounds are frequently used in lubricating oil additives [15]. The concentration of elemental components in diesel soot generally varies with operating conditions, which affect fuel and oil consumption, combustion efficiency (soot production), and mechanical strain [12].

SEM Analysis of Particulate Morphology:
There were some very evident changes of the microstructure of the diesel particulate samples. The structures of the diesel particulates are apparent from the images shown in Figures 5 and 6 for the samples collected from the exhaust of the diesel engine. The samples are seen to consist of primary particles (soot) agglomerated into aggregates (particulate). The particles range in appearance from clusters of spherules to clusters of platelets. The clusters may contain as many as 100 spherules, which range in diameters between 30 and 150 nm. The clusters of spheres are considered to be solid carbon (soot). Particulate matter is a combination of solid carbon particles surrounded by insoluble as well as soluble hydrocarbons [16]. What is seen in Figures 6 (a)-(d) is mostly the carbon particles. Whereas in Figure 5(d), what is seen is the substantial agglomeration of the primary soot particles which are bound together by condensable hydrocarbons. In other words, Figure 5(d) shows particulate matter from an engine operating condition where the oxidation of condensable hydrocarbons is poor. Enhanced oxidation of the SOF during the combustion process would leave a more porous and less agglomerated particulate structure [17]. Furthermore, under the conditions of Mode 4 (see Figure 5(d)), the engine releases particulates in a form that is potentially harmful to the environment and human health, since it is known that the condensable (and mostly soluble) fraction of the particulate contains known and suspected carcinogens [16].

Thermal Analysis of Diesel Particulates:
Thermal analysis of diesel particulate matter yields the boiling point distribution of its volatile components. It is important to bear in mind that the R&P Series 5100 differs from a conventional TGA apparatus in that it does not weigh the sample as it is heated but measures the amount of CO_2 formed when carbonaceous materials are oxidized.

For comparative purposes, the data are plotted in Figure 7 (a)–(d). It can be seen that particulates from the ceramic-coated engine contain 13–60% less low-to-medium boiling hydrocarbons than do particulates from the baseline engine. The source of these hydrocarbons is believed to be unburned fuel [17]. The material evolved between 300-450° C consists of high-boiling components, likely from the lubricating oil, and does not seem to be affected very much by the ceramic insulation. The dry soot fraction of the particulate is much higher across all the operating modes for the ceramic-coated engine. It is clear that the particulates from the ceramic-coated engine have a lower volatile content. The lower volatile content reduces the degree to which soot particles agglomerate into larger structures [18]. The particulate carbon concentrations in the exhaust are also shown in Figure 4. It is clear that the ceramic coating caused a reduction in the total particulate emissions.

Thermogravimetric analysis of fresh and used SAE 10W30 lubricating oil was also performed using a Mettler TA4000 Thermal Analyzer. The analysis was done in air at 5°C/min with a sample weight of approximately 22 mg. It was found that a little over 10% of the oil volatilizes before 250°C. The cylinder liner temperature in a conventional diesel engine is about 150°C near top dead center (TDC) and decreases significantly with distance from the cylinder head [16]. The cylinder liner temperature in a ceramic-coated engine would have to be over 100°C

higher to result in greater consumption of lubricating oil relative to the baseline engine. Also, very little difference in thermal stability was found between the fresh and used oils. The used oil was collected after about 60 h of engine operation.

With an uncooled or insulated liner, the full load increase in cylinder liner temperature near TDC can be 100°C or higher. Higher liner temperatures frequently result in lubrication problems due to increased oil consumption and lower volumetric efficiency due to heat transfer to the intake air. For this reason, it is generally preferred to leave the liner cooled and uninsulated. Alkidas [14] found a significant increase in the volatile fraction of the particulates emitted by an uncooled engine with an air-gap insulated piston, fore deck, and exhaust ports. Sudhakar and Hunter [18] reported that the dry soot emission from an uncooled engine is lower, but the extractable mass is higher by as much as 50%. In both cases, increased lubricating oil consumption was suggested as the reason for the higher volatile content. Since both groups used an uncooled cylinder liner, the higher liner temperatures may indeed have resulted in increased evaporation of oil from the liner surface.

In this work, the cylinder liner was left cooled and uninsulated. The average coolant temperature was 110° C for both baseline and ceramic-coated engines. Across all the operating modes, the ceramic-coated engine produced particulates with more dry soot and fewer volatiles. The lubricating oil contribution was relatively unaffected, suggesting that the liner temperature did not change very much. The compositional differences between particulates from the two engines can be attributed to differences in the engine exhaust conditions [12]. At exhaust temperatures above 500° C, the particles are composed principally of carbon coated with some hydrocarbons. As the temperatures decrease below 500° C, the particles become increasingly coated with condensed and adsorbed high molecular weight hydrocarbons. Figure 8 shows the exhaust temperature at different powers for the baseline and ceramic-coated engine configurations. At Mode 1 (highest power), the exhaust temperature for the insulated engine is about 520° C – almost 70° higher than the baseline engine. The hotter exhaust results in less hydrocarbon condensation and increased post-cylinder (manifold) oxidation of hydrocarbons. Therefore, the decrease in the volatile portion of the particulate matter is attributed to the higher exhaust temperature. This result is in contrast to the observations of Voss et al., who saw an overall reduction in total particulates, but observed an increase in the volatile fraction of the remaining particulate matter (i.e., a decrease in the dry soot fraction) as a result of thermal barrier coated engine components [4].

CONCLUSIONS

A combination of particulate mass, microscopic, and thermal analyses suggest that ceramic insulation of the combustion chamber walls of an IDI diesel engine is effective in reducing the volatile portion of the particulate emissions. The hotter exhaust condition in the ceramic-coated engine decreases the tendency for vapor phase hydrocarbons to condense on the particulates, resulting in a lower volatile fraction and a lower total particulate mass. With a cooled cylinder liner, no increase in the lubricating oil contribution to the volatile fraction was found relative to the baseline engine. The results indicate that it may be desirable to maintain cooling of the liner to keep oil consumption to a minimum. Thus, the original concept of the low heat rejection engine (increased thermal efficiency by decreased heat rejection) may not have proven viable. But, the thermal barrier coated engine can prove useful as one route to cleaner burning diesel engines.

ACKNOWLEDGMENTS

The authors wish to thank the U.S. Coast Guard R&D Center for support of this work. Also, the authors wish to acknowledge in-kind support from Dr. Rafal Sobotowski of BP Oil Co., who supplied the fuel used in this study.

REFERENCES

1. Amann, C. A., "Promises and Challenges of the Low-Heat-Rejection Diesel, "J. *Engr. Gas Turbines Power,* 110:475-481 (1988).

2. Belardini, P., Bertoli, C., Corcione, F.E., and Police, G., "Thermal Barriers Adoption in D.I. Diesel Engines: Effect on Smoke and Gaseous Emissions," SAE Paper No. 840995 (1984).

3. Siegla, D. C. and Alkidas, A. C., "Evaluation of the Potential of a Low-Heat-Rejection Diesel Engine to Meet Future Heavy-Duty Emissions Standards," SAE Paper No. 890291 (1989).

4. Voss, K., Cioffi, J., Gorel, A., Norris, M., Rotolico, T., and Fabel, A., "Zirconia Based Ceramic, In-Cylinder Coatings and Aftertreatment Oxidation Catalysts for Reduction of Emissions from Heavy Duty Diesel Engines," SA EPaper No. 970469 (1997).

5. Marks, D.A. and Boehman, A.L., "The Influence of Thermal Barrier Coatings on Morphology and Composition of Diesel Particulates," SAE Paper No. 970756 (1997).

6. Boehman, A. L., Vittal, M., Borek, J. A., Marks, D. A. and Bentz, A. P., "The Effects of Thermal Barrier Coatings on Diesel Engine Emissions," to be presented at the 1997 Fall Technical Conference of the ASME Internal Combustion Engines Division, Madison, WI, Sept. 27-Oct. 1 (1997).

7. Vittal, M., Borek, J. A., Boehman, A. L. and Okrent, D. A., "The Influence of Thermal Barrier Coatings on the Composition of Diesel Particulate Emissions," to be presented at the 1997 Fall Fuels and Lubricants Meetings of the SAE, Tulsa, OK, Oct. 13-16 (1997).

8. Megnin, M. K and Choate, P. J., "Combustion Chamber Deposit Measurement Techniques," SAE Paper No. 940346 (1994).

9. Thring, R.H., "Low Heat Rejection Engines," SAE Paper No. 860314 (1986).

10. Dickey, D.W., "The Effect of Insulated Combustion Chamber Surfaces on Direct Injected Diesel Engine Performance, Emissions and Combustion," SAE Paper No. 890292 (1989).

11. Assanis, D., Wiese, K., Schwarz, E. and Bryzik, W., "The Effects of Ceramic Coatings on Diesel Engine Performance and Exhaust Emissions," SAE Paper No. 910460 (1991).

12. Heywood, John B., Internal Combustion Engine Fundamentals. McGraw-Hill, New York (1988).

13. Arnann, C. A., "The Low-Heat-Rejection Diesel (Also Called the 'Adiabatic Diesel')," in Advanced Diesel Engineering and Operation, ed. S. D. Haddad, Ellis Horworth, Chichester, UK, pp. 173-239 (1988).

14. Alkidas, A.C., "Performance and Emissions Achievements with an Uncooled Heavy Duty Single Cylinder Diesel Engine," SAE Paper No. 890144 (1989).

15. Amann, C. A. and Siegla, D. C. "Diesel Particulates - What They Are and Why," *Aerosol Science Technology,* 1:73-101 (1982).

16. Neeft, J. P. A., Makee, M., and Moulijn, J. A., "Diesel Particulate Control," *Fuel Processing Technology,* 47:1-69 (1996).

17. Ishiguro, T., Suzuki, N., Fujitani, Y., and Morimoto, H., "Microstructural Changes of Diesel Soot During Oxidation," *Combustion and Flame, 85:1-6* (199 1).

18. Sudhakar, V. and Hunter, G., "Transient Emissions from an Uncooled Diesel Engine." SAE Paper No. 860224 (1986).

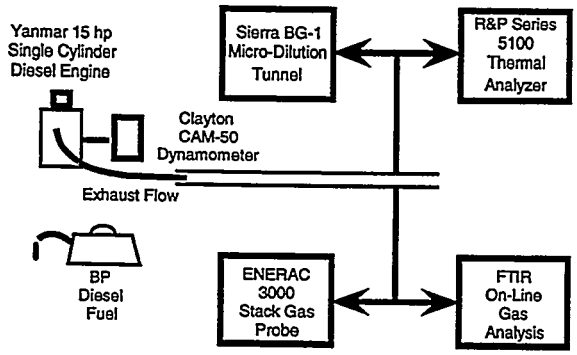

Fig. 1 Schematic of the single-cylinder engine test cell

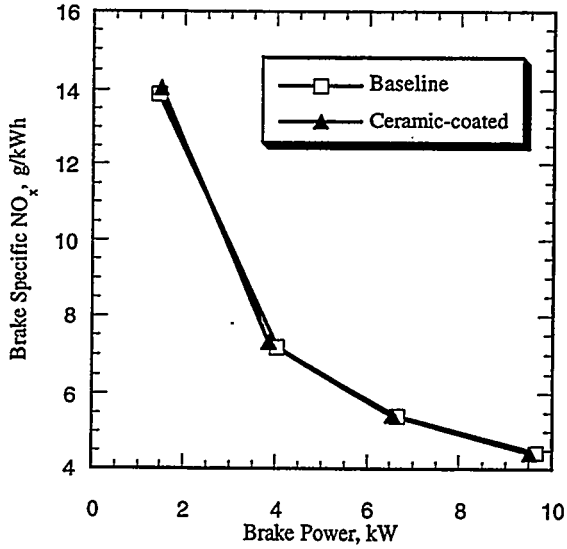

Fig. 3 Brake specific NO_x emissions for the baseline and ceramic-coated engine configurations.

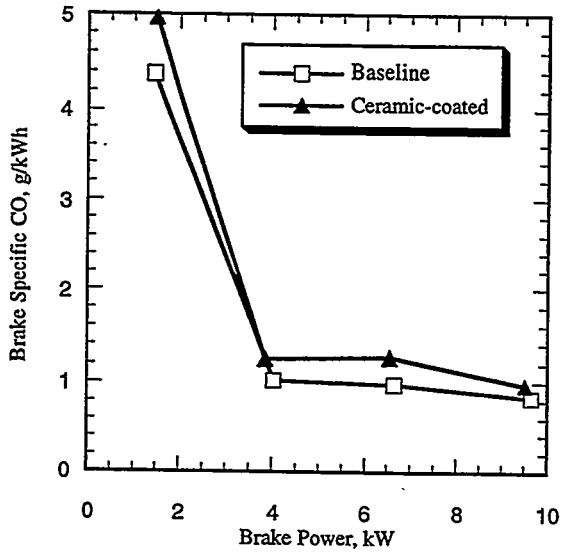

Fig. 2 Brake specific CO emissions for the baseline and ceramic-coated engine configurations.

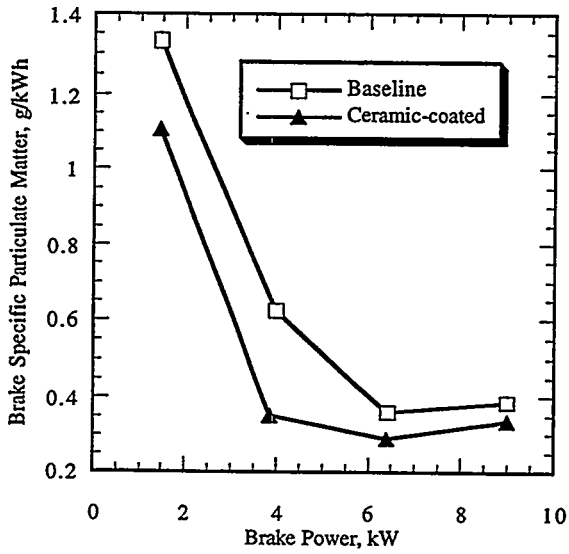

Fig. 4 Brake specific particulate matter emissions for the baseline and ceramic-coated engine configurations.

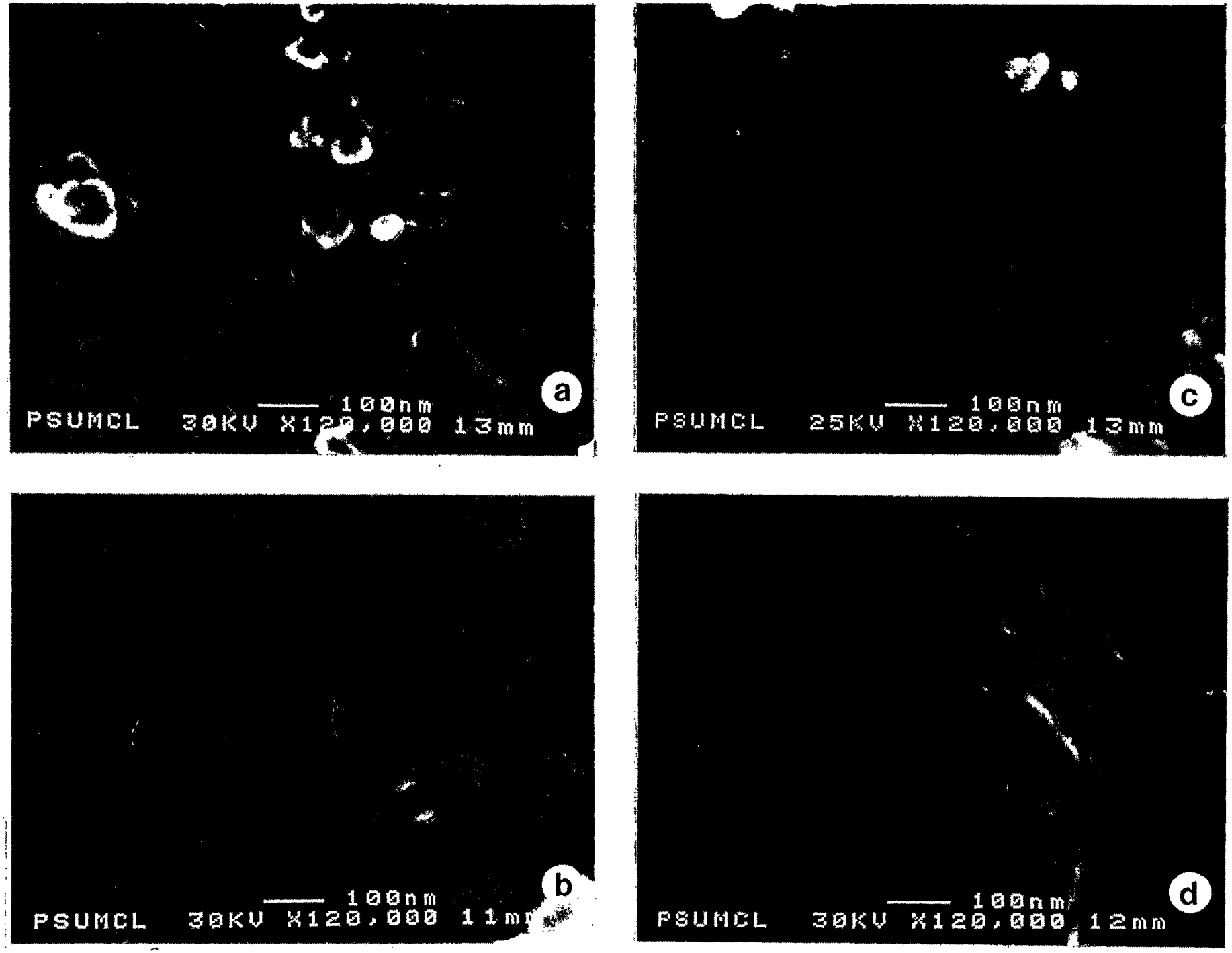

Fig. 5 SEM Micrographs at 120,000x magnification for the baseline engine configuration: (a) Mode 1; (b) Mode 2; (c) Mode 3; (d) Mode 4.

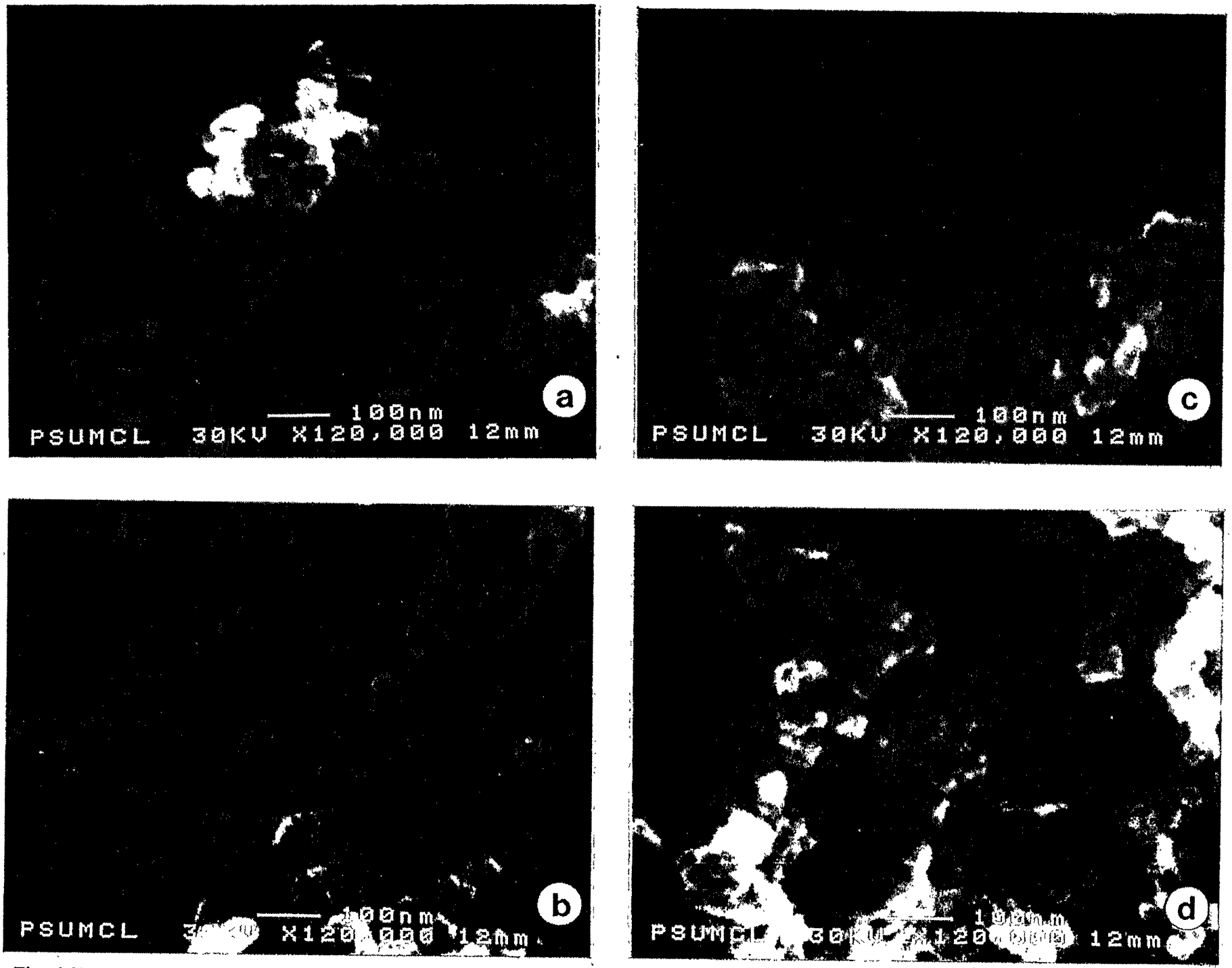

Fig. 6 SEM Micrographs at 120,000x magnification for the ceramic-coated engine: (a) Mode 1; (b) Mode 2; (c) Mode 3; (d) Mode 4.

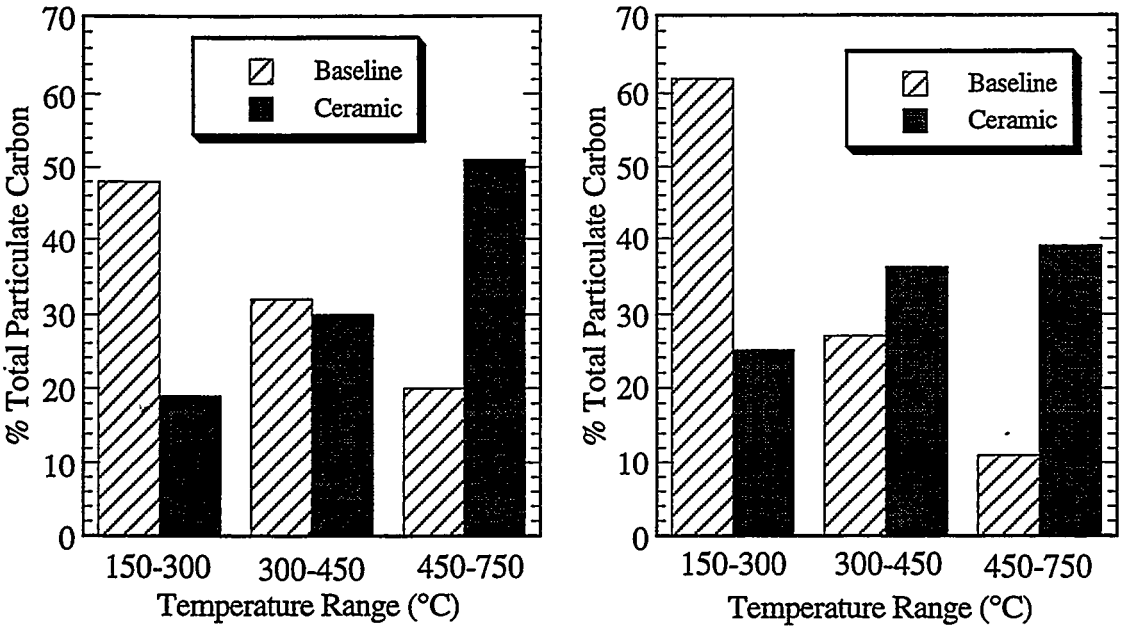

(a) Mode 1

(c) Mode 3

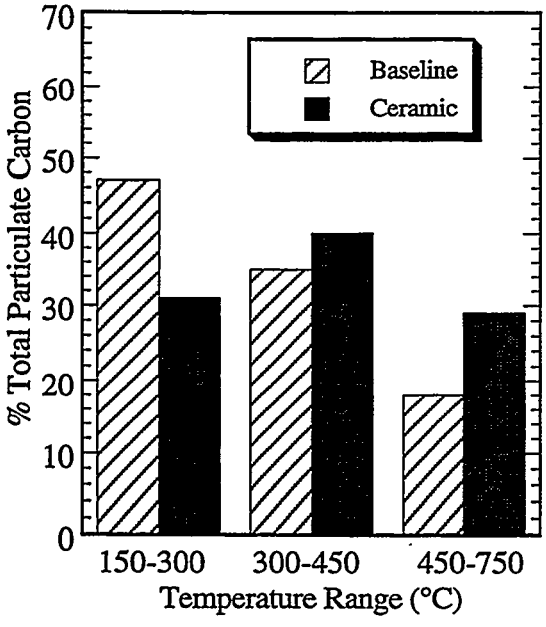

(b) Mode 2

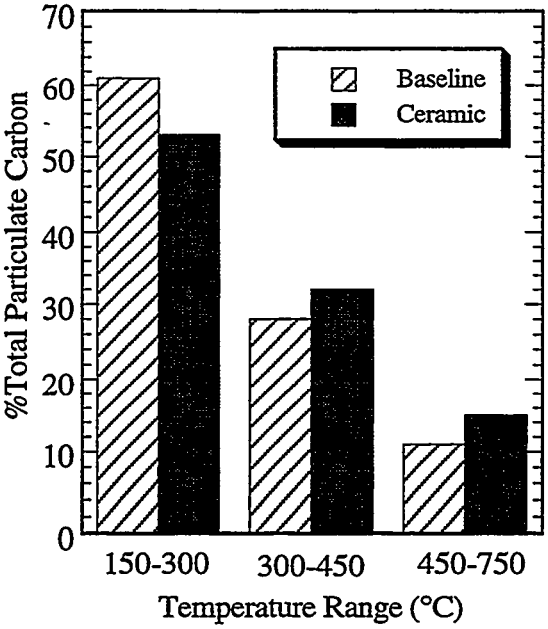

(d) Mode 4

Fig. 7 Compositional changes between particulate matter determine by thermal analysis for the baseline and ceramic-coated engine configurations.